

Studies on effect of particle size on sensitivity and decomposition of hexogen

Sanjay Vishwasrao Ingale^{*†}, Pratap Baburao Wagh^{*}, Amit Rav^{**}, and Trilok Chand Kaushik^{*}

^{*}Homi Bhabha National Institute Deemed University, Mumbai, INDIA

Phone: +91-222559-1808

[†]Corresponding author: svingale@barc.gov.in

^{**}Applied Physics Division, Bhabha Atomic Research Centre, Trombay, Mumbai -400085, INDIA

Received: March 15, 2019 Accepted: October 2, 2019

Abstract

Effect of particle size on energetic properties of Hexogen has been studied. To have a comprehensive picture, a wide range of particle size from 126 μm to 55 nm obtained by processing Hexogen with different techniques has been studied. Using sol-gel method, Hexogen materials with nanometer size particles have been prepared with induced defects like porosity. Chemical structure of processed materials with reduced particle size is found to be similar to that of raw material but these materials were having more uniform morphology with regular shaped particles. Kinetic parameters derived from thermal analysis indicated increase in activation energy with decrease in particle size, however, increase in rate constant suggested faster decomposition and higher energy release rate in these materials. Increase in detonation velocity of these materials supported observations noted in kinetic parameters study. Impact sensitivity was found to be decreased with decrease in particle size except for sol-gel processed samples. Though, activation energy in sol-gel processed samples was found to be increasing, impact test studies on these materials showed significant increase in sensitivity even though the particle size is reduced. This indicates that decomposition mechanism on impact in these samples is significantly affected by the defects like porosity.

Keywords: energetic materials, hexogen, ultrafine particles, thermal decomposition, kinetics

1. Introduction

Energetic materials offer compact sources of high energy density with important applications for various military, civil and research purposes. In development of such materials, a major objective is to have desired control on sensitivity to initiation and energy release rate. For this it is imperative to understand the behavior of these materials. The inadvertent initiation of energetic materials can basically occur due to energy received from impact or heat stimuli. Thermal initiation of energetic materials is also an important aspect as initiation by any external stimuli result in thermal decomposition of energetic materials¹⁾. The energetic properties are believed to depend upon micro structure, particle size, surface area and defects in the material²⁾. Among these variants, particle size can be effectively controlled to modify the properties of the energetic materials³⁾. Several researchers have attempted to study effect of particle size

on sensitivity of the energetic materials, but no clear trends have emerged or agreed upon. Interestingly, the results are seen to be contradictory showing both the trends of increase as well as decrease in sensitivity to initiation of explosives as the particle size is reduced from coarser to fine. For example, Fathollahi *et al.*⁴⁾ reported that activation energy of micron size RDX is 1.5 times higher than that for nano RDX whereas Huang *et al.*⁵⁾ reported that nano size FOX-7 material has higher decomposition temperature than micron size material. The reason for this could be that these studies have been conducted on materials with different processing history and having different range of particle size distribution. The different techniques like thermal or impact initiation used to measure sensitivity properties or the parameters considered as measure of ignition may also give different results and therefore these results are inadequate to lead to some conclusion. The processing method may also

affect decomposition phenomenon⁶). Therefore, investigating the effect of particle size on the sensitivity of energetic materials to initiation is of great interest.

In present work, we studied the effect of particle size on thermal and impact sensitivity of Hexogen, popularly known as RDX and whether improvement in performance can be achieved by reducing its particle size. Hexogen materials with variation in particle size ranging from 126 micrometer to 55 nanometers were prepared. The effect of porosity was also been studied for material processed by sol-gel method. The processed materials were characterized with infra red spectroscopy, scanning electron microscopy and thermal analysis. The impact sensitivity and detonation velocity measurements were also carried out.

2. Experimental

Hexogen was received in powder form from ordnance factory. The chemicals acetone, dimethylformaldehyde (DMF) and hydrofluoric acid were of analytical grade. Tetramethylorthosilicate (TMOS) was from Fluka. Double distilled water was used for preparation of catalyst and also as non-solvent for Hexogen.

Raw Hexogen, as received, was used as one of the particle size under study. It was processed using solvent non-solvent precipitation method⁷ and spray drying method⁸ to reduce the particle size. In solvent non-solvent precipitation method, Hexogen was dissolved in acetone in 1:15 ratio by weight. The solution was then added to water that resulted in precipitation of Hexogen. The precipitated Hexogen was separated from water by filtration and dried in oven at 70 °C.

In spray drying method, Hexogen was dissolved in DMF. Hexogen to DMF ratio was optimized to 1:6 by weight. The solution was sprayed in a heated chamber with feed rate at 1 mL min⁻¹. The temperature at inlet of the chamber was maintained at 160 °C. The solvent from fine droplets evaporated, resulting in crystallization of Hexogen particles.

The Hexogen was also processed by sol-gel method using silica (SiO₂) as host matrix⁹. In this method, raw Hexogen was dissolved in acetone. Amount of Hexogen was chosen so as to obtain 90% Hexogen in Hexogen/SiO₂ composite. To this solution, TMOS and water was added. The weight ratio of TMOS: Acetone: Water was 1:40:4. This solution transformed to gel with Hexogen having entrapped in gel pores. The gel was dried at ambient conditions resulting in Hexogen/SiO₂ composite.

Infrared spectroscopy measurements were carried out on Bruker make FTIR spectrophotometer using attenuated total reflection technique. Powder samples of about 3–5 mg were scanned within the wave number range of 550 to 5000 cm⁻¹.

The morphology of the Hexogen material was studied using Carl Zeiss Auriga Field Emission Scanning Electron Microscope (FESEM). For FESEM, the Hexogen powder was dispersed on carbon film and then gold coated.

The kinematic studies were conducted by Thermo gravimetric (TG) and differential scanning calorimetric

(DSC) analysis. TG-DSC measurements were carried out from room temperature to 300 °C with dry N₂ as carrier gas at flow rate of 20 mL min⁻¹. The samples of about 1 mg were heated in alumina crucibles at different heating rate of 5, 10 and 20 °C min⁻¹.

Impact sensitivity studies were carried out by Fall Hammer Impact Test using 2 kg weight. The powder sample of about 30–40 mg was placed on anvil and the height of impact (2 kg hammer) was varied as per Bruceton up-down method to arrive at a height with 50% probability of initiation.

Experimental assembly for detonation velocity measurement consisted donor charge and acceptor charge along with three self shorting sensors that are placed at three different locations. Donor charge was 5 mm thick and 20 mm diameter PETN pellet and it was initiated using electrical detonator. To detect the initiation of donor charge, a self shoring sensor 'S1' is placed on the surface of the donor charge. To measure the detonation velocity of the acceptor charge (10 mm thick and 20 mm diameter pellets of hexogen materials), two self shorting sensor 'S2' and 'S3' are used. Sensor 'S2' is placed 3 mm deep inside the acceptor charge from the rear surface and sensor 'S3' is placed on the rear surface of the same charge. Sensor output on the oscilloscope record indicates the arrival of detonation wave front at the sensor location. Detonation velocity is then, calculated by knowing the travel time of detonation front between two sensor location. In present case the output of three sensors ('S1', 'S2' and 'S3') is multiplexed in one output where each step indicates individual sensor and amplitude of step is the identification of the sensor (e.g. 'S1' is 1.8 V, 'S2' is 1.2V and 'S3' is 0.7V, respectively). The measurement was repeated two times for each of Hexogen material with different particle size.

3. Results and discussions

3.1 FTIR spectroscopy

FTIR characterization was carried out to look for any change in chemical structure of processed material. Figure 1 shows FTIR spectra for Hexogen processed by different techniques. In all spectra, peaks observed at 1045 cm⁻¹ correspond to C-N stretching ring and peaks observed at 1268 and 1596 cm⁻¹ attributed to symmetrical N-N vibration and anti symmetrical NO₂ vibrations, respectively¹⁰. These bands are typical signature of Hexogen. In IR spectra of sol-gel processed Hexogen material Figure 1(d), indication of absorption bands at 1100 cm⁻¹ is observed which correspond to Si-O vibration in silica. There is no change or shift in Hexogen absorption bands in IR spectra which indicates that chemical structure of processed Hexogen is same to that of raw Hexogen.

3.2 FESEM

The FESEM images of the raw Hexogen and Hexogen processed by different techniques are shown in Figure 2. The particle sizes are carefully measured from the micrograph to obtain particle size distribution. The raw Hexogen particles are irregular in shape having sharp

edges or horns Figure 2(a) with particle size in the range of $126 \pm 45 \mu\text{m}$. In material processed by solvent precipitated method, particle size is much smaller as compared to raw hexogen and is in the range of $4.37 \mu\text{m} \pm 2 \mu\text{m}$. Particles are uniform with a few rod shaped particles where the sharp edges are reduced Figure 2(b). Micrograph in Figure 2(c) displays material processed by spray drying method. It shows that the particles are nearly spherical in shape and uniform in size in the range of 194 ± 63 nanometers. In Hexogen/SiO₂ composite Figure 2(d), though Hexogen and SiO₂ phases cannot be resolved from one another, the overall small spherical

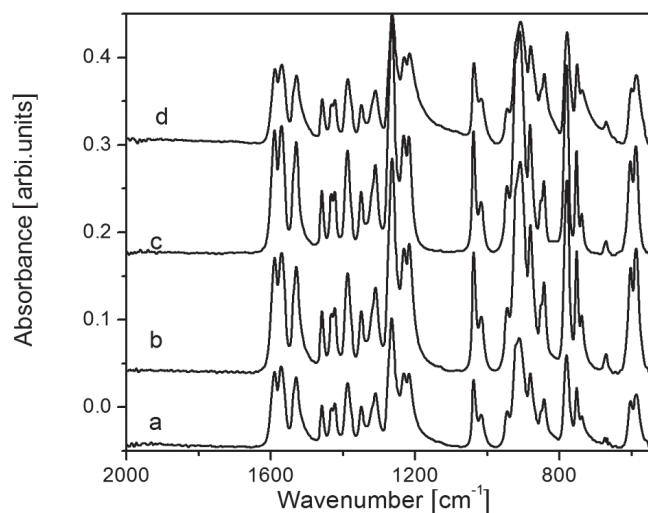


Figure 1 IR spectra for a) raw Hexogen and Hexogen processed by b) solvent precipitation, c) spray drying and d) sol-gel method.

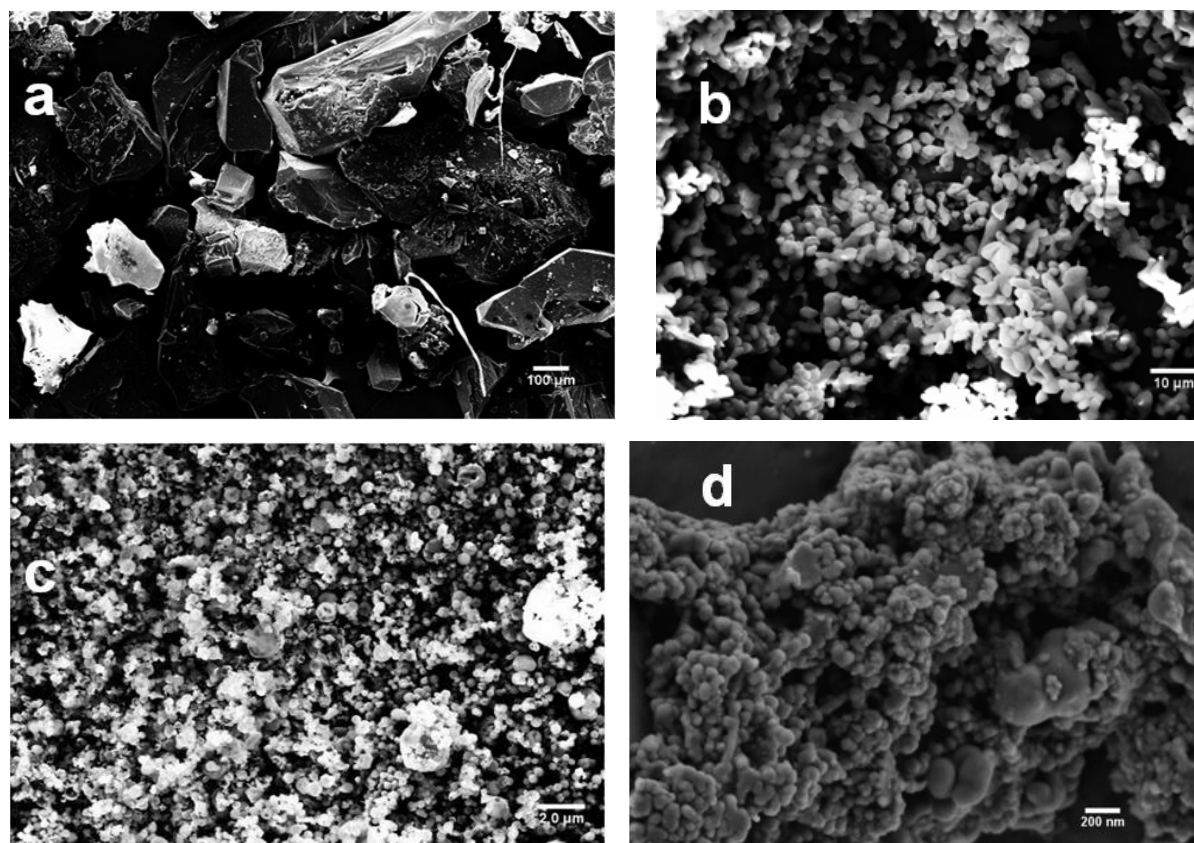


Figure 2 FESEM of a) raw Hexogen, and Hexogen processed by b) solvent/non solvent precipitation, c) spray drying and d) sol-gel method.

particles of both the constituents are in nanometer range. Particles size is in range of 55 ± 25 nm. Particles are well connected resulting in porous microstructure of interconnected clusters. Based on particle size, raw Hexogen and Hexogen processed by solvent precipitation, spray drying and sol-gel method have been designated as Hexogen (126), Hexogen (4.37), Hexogen (0.194) and Hexogen (0.055), respectively.

3.3 TG-DSC

Figure 3 shows the TG-DSC curves for Hexogen materials heated from room temperature to 300 °C at heating rate of 5, 10 and 20 °C min⁻¹. The sudden weight loss in TG curves of all samples at around 220 to 260 °C is associated with thermal decomposition of Hexogen. TG curves of Hexogen other than Hexogen (0.055) i.e. Hexogen-SiO₂ composite show mass loss of about 99%. In Figure 3(d), Hexogen (0.055) shows mass loss of around 88% indicating major content is Hexogen with rest of non-energetic residue (silica) that agrees well to our precursor composition.

In DSC curves, the endotherm at about 205 °C is associated with melting of Hexogen followed by an exotherm attributed to its decomposition. At higher heating rate, exothermic peak is shifted towards higher temperature in all the samples. The energy associated with exothermic peak during decomposition is also more at higher heating rate. The kinetic of decomposition process is function of temperature and time, therefore, peak temperature shifted to higher value with increase in heat of reaction. Change in heating rate may change

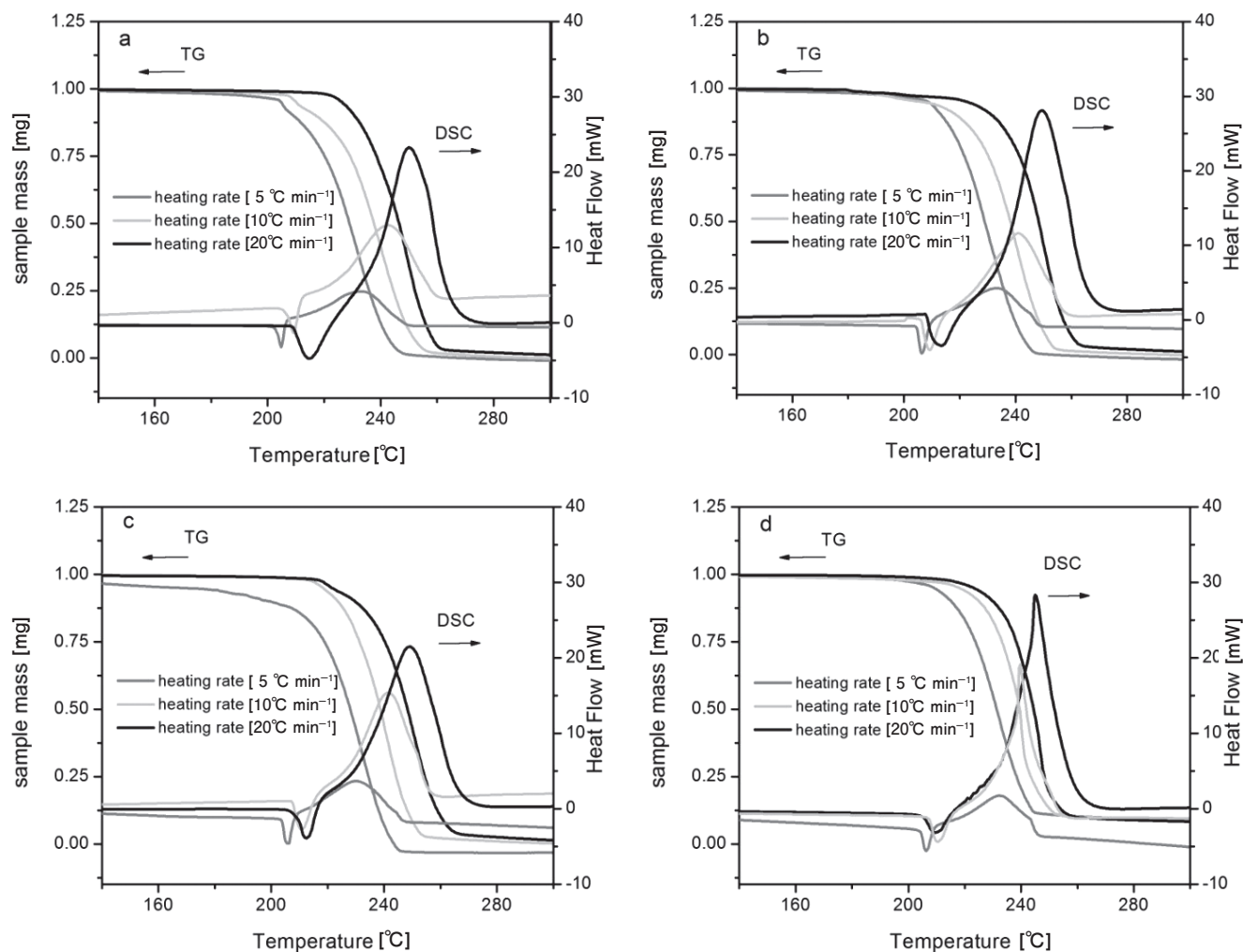


Figure 3 TG-DSC curves for a) Hexogen (126), b) Hexogen (4.37), c) Hexogen (0.194) and d) Hexogen (0.055).

Table 1 Exothermic peak temperature (T_p) and Onset Temperature (T_o) for Hexogen materials at different heating rate.

Heating rate β [°C min ⁻¹]	Exothermic peak temperature (T_p) and Onset Temperature (T_o) for Hexogen processed by different techniques [°C]							
	Hexogen (126)		Hexogen (4.37)		Hexogen (0.194)		Hexogen (0.055)	
	T_p	T_o	T_p	T_o	T_p	T_o	T_p	T_o
5	233	212	232.6	212	231.2	215	231.1	220
10	242.5	215	241.2	217.5	241.0	220	240.2	225
20	251.1	220	250.4	223	249.1	225	246.5	233

degree of reactivity during that time and may cause overlapping of thermo kinetic events resulting in high heat of reaction¹¹). The exothermic peak temperature and onset temperature obtained from DSC curve is shown in Table 1.

Hexogen material with reduced particle size show shift in exothermic peak towards lower temperature. Many researchers have reported that the shift in peak temperature to lower value indicates increase in sensitivity of energetic materials with reduced particle size. However, in some reports, the transition from thermal decomposition to thermal explosion is assumed to begin at onset temperature where increase in rate of change in heat flow is observed. As noted from the values

of Table 1, the onset temperatures is found to be shifted at relatively higher temperature in the Hexogen materials with reduced particle size as compared to that of Hexogen (126). It suggests the decrease in sensitivity with reduced particle size. This appears to be the reason for difference in interpretation of thermal initiation. We tried to separate the ignition phenomenon and ignition to explosion transition on basis of kinetic parameters. The higher values of onset temperature in materials with reduced particle size may be related to higher activation energy whereas the shift in exothermic peak temperature to lower value is due to the fact that these materials have larger proportion of atoms located on surface and enhancement in surface area that leads to increase in

Table 2 Kinetics parameters for Hexogen material derived from TG-DSC curves.

Hexogen material	Average particle size	Kinetics		
		E_a [kJ mol ⁻¹]	Z [s ⁻¹]	$k \times 10^{-2}$ [s ⁻¹]
Raw	126 ± 45 [μm]	149 ± 3	4.7 × 10 ¹⁵	69 ± 1
Solvent precipitated	4.37 ± 2 [μm]	159 ± 7	1.4 × 10 ¹⁶	72 ± 1.5
Spray dried	194 ± 63 [nm]	176 ± 7	6.5 × 10 ¹⁷	81 ± 1.5
Sol-gel processed	55 ± 25 [nm]	215 ± 9	8.0 × 10 ²¹	98 ± 2.1

reactivity and faster decomposition.

In kinetic measurements, activation energy (E_a), Pre exponential factor (Z) and decomposition rate (k) are important parameters. In energetic materials, decomposition rate usually depends only upon temperature and thermally stimulated decomposition process may be described¹²⁾ by Equation (1).

$$k(T) = Z \exp(-E_a/RT) \quad (1)$$

Where E_a is in J, R is gas constant in J K⁻¹ mol and T is temperature in K.

The value of E_a was evaluated from exothermic peak temperature obtained with various heating rates as shown in Table 1 and applying Kissinger's method¹³⁾.

$$-E_a/R = d \ln(\beta/T_p^2) / d(1/T_p) \quad (2)$$

$$\ln(\beta/T_p^2) = \ln(ZR/E_a) - (E_a/RT_p) \quad (3)$$

Where β is the heating rate in K min⁻¹ and T_p is the maximum temperature of DSC curve for that heating rate in K.

The values of E_a obtained from the slope of the straight line of plot $\ln(\beta/T_p^2)$ against $1/T_p$ are listed in Table 2. The activation energy for Hexogen (126) is close to the reported value¹⁴⁾. E_a for the Hexogen materials with reduced particle size were found higher than that of raw material with coarse particle size. Heat buildup in energetic materials depends upon temperature as well as its thermal conductivity. With reduced particle size, surface losses and thermal conductivity is more. Therefore, it requires higher temperature to trigger ignition (onset in DSC curve) as indicated by high activation energy with reduced particle size. In Hexogen-SiO₂ composite, Hexogen is surrounded by silica because of which higher temperature is required to heat and ignite Hexogen in these materials. It is supported by significant high activation energy observed in this material.

From DSC curves, the reactivity and decomposition rate is anticipated to improve with reduced particle size. To explain this, Z and k are calculated using Equation (1) and (3) and are listed in Table 2. Z represents the frequency of collisions and k represents reaction rate constant. The Z and k values for Hexogen with reduced particles size are higher than that of relatively coarser materials. It may be attributed to more number of atoms undergoing decomposition simultaneously due to high proportion of surface atoms with reduced particle size. These are in vicinity of large number of other particles which in turn increase the collision frequency. It is evident from high values of Z and k for Hexogen (4.37) and

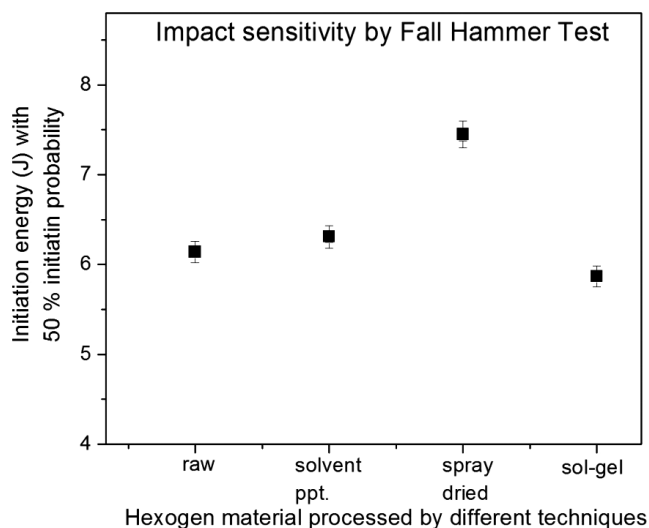


Figure 4 Impact sensitivity data for Hexogen materials processed by different techniques.

Hexogen (0.194). High surface energy associated with smaller size particles also contributes to faster decomposition, once it is initiated. Moreover, in Hexogen (0.055), due to high onset temperature as noted in Table 1, decomposition reaction favours more NO₂ and CO₂ contributing to more energy release accelerating the reaction rate¹⁾. As shown in Figure 3(d) the shape of exothermic peak for Hexogen material processed by sol-gel method becomes steeper towards the top which indicates that an additional mechanism through void collapse assists to increase the reaction rate with high defect density. Increase in Z and k values suggests a possible improvement in detonation velocity of Hexogen with reduced particle size.

3.4 Impact sensitivity measurements

Results of impact sensitivity measurements carried out using BAM fall hammer test on the Hexogen materials are shown in Figure 4. Impact sensitivity was found to be decreased with reduced particle size for Hexogen (4.37) and Hexogen (0.194) as compared to that of Hexogen (126). It may be due to reduced crystal defect and voids in materials with reduced particle size. Moreover, as seen from SEM, Hexogen (126) has more surface complexity with sharp edges. It leads to plastic deformation and cause to increase in sensitivity on impact. Hexogen (4.37) and Hexogen (0.194) have smooth surface and near spherical geometry with reduction in particle size. Therefore, these materials are less sensitive to impact. For Hexogen (0.055), the impact energy with 50% initiation probability is less

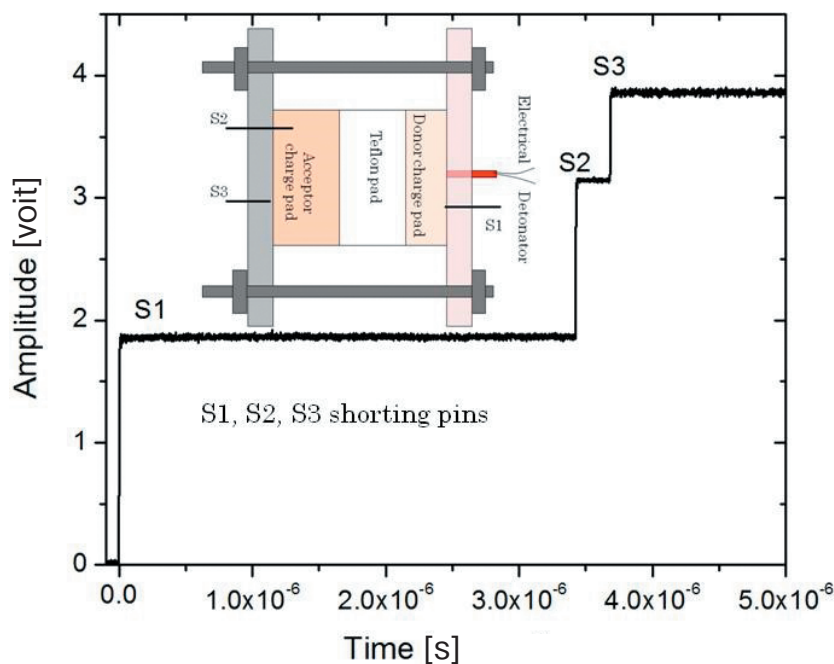


Figure 5 Experimental assemblies for detonation velocity measurement and typical velocity measurement profile for Hexogen material.

Table 3 Detonation velocity for Hexogen material with different particle size.

Hexogen material	Average particle size	Detonation velocity
Raw	126 ± 45 [μm]	7.89 ± 0.2 [mm μs ⁻¹]
Solvent precipitated	4.37 ± 2 [μm]	8.26 ± 0.2 [mm μs ⁻¹]
Spray dried	194 ± 63 [nm]	8.89 ± 0.2 [mm μs ⁻¹]
Sol-gel processed	55 ± 25 [nm]	8.12 ± 0.2 [mm μs ⁻¹]

than that of Hexogen (126) implying that these samples are more sensitive even though particle size is much smaller as compared to that of other samples. Impact initiation in energetic materials occurs through hot spots by localizing incident energy¹⁵. The induced porosity in these materials processed by sol-gel method provides many defect centers for adiabatic compression on impact raising local temperature to ignition. The visco-plastic flow at pore-particle interface on impact shearing may provide initiation centers and lead to increase in impact sensitivity of this material.

3.5 Detonation velocity measurements

Detonation velocity measurements were conducted to support the observation from kinetic studies indicating improvement in energy release rate of Hexogen with reduced particle size. Experimental assembly and typical velocity measurement profile is shown in Figure 5. The donor charge was 5 mm thick and 20 mm diameter PETN pellet with density of 1.7 g cm⁻³. The density of the acceptor charge (10 mm thick and 20 mm diameter pellet) of Hexogen with different particle size was maintained at 1.55 g cm⁻³. The data on velocity is summarized in Table 3.

The results showed that detonation velocity increased by about 12% with reduced particle size. The detonation velocity in Hexogen (4.37) and Hexogen (0.194) is higher than that of Hexogen (126) that indicates ignition to explosion transition occurs in these materials on a shorter

time scale. Hexogen materials with reduced particle size exhibit higher activation energy for ignition suggesting higher hot spot temperature that leads to faster rate of chemical decomposition¹⁶. Faster transition to fully developed detonation may also result from a higher number density of hot spots as indicated by high value of pre-exponential factor Z . The larger surface area of fine grained materials also contributes to higher detonation velocity. In Hexogen (0.055), detonation velocity is higher than that of Hexogen (126), however, it is lower than that of Hexogen (0.194) in spite of lower particle size. It may be due to lower content of Hexogen (90%) in these materials that result in reducing the energy density.

4. Conclusions

Raw Hexogen materials with particle size in the range of 126 μm was further processed by solvent precipitation, spray drying and sol-gel method to obtain average particle size in the range of 4.37 μm, 194 nm and 55 nm, respectively. It offered wide range of particle size to study its effect of sensitivity of Hexogen. Sol-gel processing of Hexogen enabled to study effect of induced porosity on its sensitivity and performance. FTIR studies indicated no change in chemical structure of the processed material. Kinetic parameters studies showed that with reduced particle size, there is an increase in activation energy. However, increase in reaction rate constant and collision frequency result in faster decomposition and shifting of

exothermic peak to lower temperature in these materials. It helped to understand ignition process. Sensitivity to impact initiation of energetic materials is found to decrease with reduction in particle size. However, in Hexogen processed by sol-gel method, sensitivity to impact initiation increased even though having smaller particle size as compared to raw material. It indicates that initiation is affected by the defects like porosity that control ignition mechanism. Detonation velocity by about 12% and hence the performance of the energetic materials is improved with the reduction in particle size and this is found in agreement with results obtained from kinetics studies. It may be inferred conclusively from these studies that decrease in sensitivity and improvement in performance can be achieved by reducing the particle size of Hexogen. The initiation mechanism can also be controlled with induced defects.

Acknowledgement

Authors acknowledge help received from A. Ghosh and A K Sahu for FESEM. Authors thank to Ratanesh Kumar, R. P. Patel, N. Singnurkar, P. C. Das, S. L. Gavit, S. D. Virnak and S. D. Wakode for experimental assistance.

References

- 1) S. Kim, B. Nyande, H. Kim, J. Park, W. Lee, and M. Oh, *J. Hazard. Mater.*, 308, 120–130 (2016).
- 2) X. Song and F. Li, *Def. Sci. J.*, 59, 37–42 (2009).
- 3) J. Liu, L. Wang, and Q. Li, *Chin J. Explos. Propellants*, 35, 46–50 (2012).
- 4) M. Fathollahi and B. Mohammadi, *J. Mohammadi, Fuel*, 104, 95–100 (2013).
- 5) B. Huang, M. Cao, F. Nie, H. Huang, and C. Hu, *Def. Technol.*, 9, 59–79 (2013).
- 6) J. Zhang, Y. Liu, X. Zhang, Y. Fan, J. Xu, R. Wang, Y. Wang, and J. Zhang, *J. Therm. Anal. Calorim.*, 129, 733–741 (2017).
- 7) Y. Wang, X. Song, D. Song, W. Jiang, H. Liu, and F. Li, *Propellants, Explos., Pyrotech.*, 36, 505–512 (2011).
- 8) J. Kim, M. Shin, J. Kim, H. Kim, and K. Koo, *Ind. Eng. Chem. Res.*, 50, 12186–12193 (2011).
- 9) S. Ingale, P. Wagh, P. Sastry, C. Basak, D. Bandyopadhyay, S. Phapale, and S. Gupta, *Def. Technol.*, 12, 46–51 (2016).
- 10) A. Pant, A. Nandi, S. Newale, V. Gajbhiye, H. Prashanth, and R. Pandey, *Cent. Eur. J. Energ. Mater.*, 10, 393–407 (2013).
- 11) Y. Yu, S. Chen, T. Li, S. Jin, G. Zhang, M. Chenb, and L. Li, *RSC Advances*, 7, 31485–31492 (2017).
- 12) H. Pouretedal, S. Damiri, P. Nosrati, and E. Ghaemi, *Def. Technol.*, 14, 126–131 (2018).
- 13) M. Abd-Eeghany, A. Elbeih, and S. Hassanein, *Cent. Eur. J. Energ. Mater.*, 13, 714–735 (2016).
- 14) J. Lee, C. Hsu, and C. Chang, *Thermochim. Acta*, 392, 173–176 (2002).
- 15) Y. Wang, X. Song, D. Song, C. An, J. Wang, and F. Li, *Nanomater. Nanotechnol.*, 6, 1–10 (2016).
- 16) C. Tarver and S. Childester, *J. Phys. Chem.*, 100, 5794–5799 (1996).